FACIES VARIATION, MINERALOGICAL AND GEOCHEMICAL CHARACTERIZATION OF THE LOKOJA AND PATTI FORMATIONS, SOUTHERN BIDA BASIN: IMPLICATIONS FOR PROVENANCE, TECTONIC SETTING AND PALEO-CLIMATIC ENVIRONMENTS

Supported by tetfund TERTIARY EDUCATION TRUST FUND

Bankole, S.I., Opatola, A. O., Akinmosin, A., Olajuyin, J.O., Onyenwe, U.H., Oloniyo, M.O.
Department of Geosciences, University of Lagos, Akoka, Lagos, Nigeria
Corresponding Author: S.I. BANKOLE
Email: sbankole@unilag.edu.ng.

Received: December 14, 2023 Accepted: March 28, 2024

Abstract: Thirteen sandstone samples of the Lokoja Formation and six Ironstone/Shale samples of the Patti Formation were subjected to Mineralogical and Geochemical Analyses to determine the provenance, tectonic settings, and paleo-depositional environments. The mineralogical studies of the concretional ironstone revealed the occurrence of siderite (Fe_2CO_3), kaolinite (Al_2O_3 $2SiO_2{\cdot}2H_2O$), quartz (SiO_2), and hematite (Fe_2O_3) with siderite, kaolinite and quartz dominating. The oxides, Fe_2O_3, SiO_2 and Al_2O_3 constitute greater than sixty-five percent (65%) of the sample's elemental oxides composition. The Shale mineralogy revealed the occurrence of kaolinite (Al_2O_3 $2SiO_2{\cdot}2H_2O$), quartz (SiO_2), hematite (Al_2O_3), and Sylvite (KCl) with kaolinite and quartz dominating. Moreover, the shale oxide results revealed SiO_2, Al_2O_3, and MgO accounted for more than seventy percent (70%) of the shale's elemental oxides. The average elemental oxides of the Lokoja Sandstone are; 61.87% SiO_2; 17.05% Al_2O_3; 3.30% Fe_2O_3; 0.63% CaO; 1.92- 3.41% Na_2O; 2.09% K_2O and 2.54% MgO. Other oxides such as P_2O_5, TiO_2, and MnO are less than 1%. The paleo-weathering conditions of the concretional Ironstone and shale samples were determined using indices such as the Chemical Index of Alteration (CIA), Chemical Index of Weathering (CIW), Index of Compositional Variation (ICV) and Plagioclase Index of Alteration (PIA). Generally, these indices reveal that the ironstones were intensely weathered and are immature. All indices, however, showed that the shale samples are matured and had gone through extensive weathering in their source area. The average CIA value of 76.52% is indicative of an intense recycling in the source area while the average MIA value of 53.03% suggests a moderate degree of weathering. The high clay matrix and feldspar content have been used to classify the sandstones as feldsparthic greywackes deposited in Semi-arid to arid climatic conditions under a basement uplifted tectonic setting. Furthermore, the paleo-environmental conditions, provenance, and tectonic settings of the Patti Formation are a mix of mafic and intermediate provenance and tectonic settings within the Active Continental Margin (ACM). The shale provenance is a mixture of felsic and an intermediate igneous rock principally within the active continental margin.

Keywords: Ahoko, Lokoja, Bida Basin, Patti, Facies, Provenance

Introduction

The Bida Basin is one of the Nigerian hinterland sedimentary basins in Nigeria. Located in central Nigeria, the basin is contiguous with the Sokoto and Anambra Basins in the Northwest and Southeast respectively (Fig.1). It has been described as a Northwest – Southeast trending intracratonic structural depression, perpendicular to the Benue Trough main axis (Ladipo et al., 1994). The basin is subdivided into the Northern and Southern sub-basins due to its basin-wide facies changes (Jones, 1958; Braide, 1992).

The fluviatile Lokoja Formation, representing the oldest sedimentary facies of the southern Bida Sub-basin lies non-conformably on the Precambrian basement complex (Braide, 1992). The mixed marine-continentally derived Patti Formation conformable overlies the Lokoja Formation. The Patti Formation consists of sandstones, mudstones, siltstones, shales and ironstones members. Field observations of the exposed marine series of the Patti Formation at the abandoned Ahoko quarry revealed the intercalating relationship between the shale and the concretional ironstones.

Diversed research work by authors such as but not limited to: Akande et al., (2005); Obaje et al., (2011); Ojo and Akande (2008); Agunleti and Salau (2015); Nton and Adamolekun (2016); Bankole et al. (2019) have been done on the Bida basin. They include but are not limited to studying its geology/stratigraphy, sedimentological characterization, petroliferous characterization (Source rock evaluation) of the basin; petrology, genesis, mineralogy, and paleo-environment of the shales from the Patti Formation. Researchers such as Adeleye (1973), Ladipo et al. (1994), and Abimbola (1997) have been concerned about the origins of the sandstone, oolitic and ironstone of the Bida Basin. Therefore, this study is aimed at delineating the mineralogical and geochemical characterization of the Lokoja and Patti Formations as exposed in Lokoja Town and Ahoko Village along the Lokoja-Abuja expressway using XRD and XRF analyses. The findings from this study will help in filling available knowledge gap through the reconstruction of the Provenance, tectonic settings and Paleo-depositional environment of the formations.

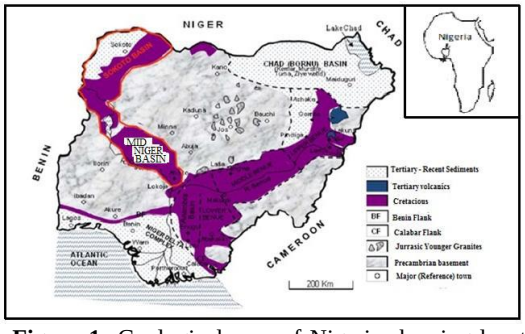

Figure 1: Geological map of Nigeria showing locations of Middle Niger Basin (After Obaje *et al*.,

Study Area Description

The study area lies within latitudes 07° 51' to 08° 26' and longitudes 006° 41' to 006° 56' (Fig. 2) and is located within Kogi State, Nigeria

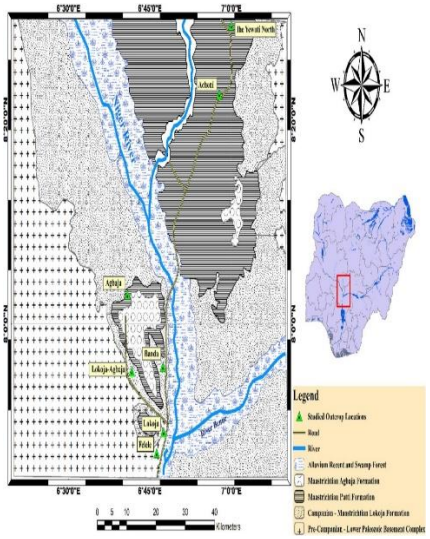

Fig. 2: Geological Map of Study Area Showing Locations of Studied Sections with Inset Map of Nigeria Showing NW/SE Trending Bida Basin (Modified After Agyingi, 1991)

Method and Techniques

Field Methods

Well-exposed stratigraphic sections of sandstone, siltstone, shale, and ironstone facies exist in the study areas. The mapping exercise was aimed at identifying the rock types and establishing stratigraphic succession of the rocks based on their field relationships. Field observations including observing grain texture, colour, grain orientation, mineralogical composition, thickness, and lateral extent of beds, taking photographs of important sedimentary structures, and logging of exposed vertical sections were done. Detailed characteristics of each bed, such as thickness, grain size, orientation, texture, colour, sedimentary structures and others were studied and documented. Fieldwork involved visits to 4 localities (Filele, Okumi, Ohono and Ahoko). The precise location of the outcrops was obtained using GPS and recorded.

A total of 36 representative samples were selected from spot samples collected for laboratory analyses including geochemical analysis and petrographic studies. A representative sample was collected for each stratum. The sediment sampling was carried out from bottom to top. Each sample collected was placed in well-labeled polythene bags with codes. The depths of each stratum were measured from bottom to top for the thickness of each stratum. Bedding characteristics in terms of texture and lithology were also studied and documented.

X-Ray Fluorescence (XRF)

Thirteen sandstone samples together with six samples of ironstones and shale were analysed at National Geoscience Research Laboratories, Nigeria Geological Survey Agency, Kaduna. XRF analysis was done using the standard method with Montana soil SRM 2710 and Thermo Fisher Scientific standard reference material. The samples were first pulverized to fine powder with the aid of mortar and pestle. Two grams (2 g) of each of the samples were weighed and then poured into a sample holder and covered with cotton wool. The bottom of the sample holder is made of polypropylene which is a thermoplastic. The sample holders containing the samples were run in a vacuum using a vacuum pump for 10 minutes to remove oxygen and moisture after which they were inserted into the XRF Spectrometer for the chemical analysis. The method was calibrated using geological calibration of oxides in a vacuum to obtain the chemical analysis result in oxides. The samples were then run in the XRF spectrometer for 10 minutes intervals. The results were obtained afterward. The determination of Loss on Ignition (LOI) was done by igniting a 1.0 g sample split at 950 °C for 90 min. The weight loss was then re-measured.

X-ray Diffraction (XRD)

The analysed samples were grounded into fine materials, and homogenized. Afterward, the powdery sample is prepared via the sample preparation block. They are then compressed in the flat sample holder to create a flat, smooth surface which is later placed on the sample stage within the XRD cabinet.

Furthermore, the reflection-transmission spinner stage using the Theta-Theta settings was used to analyze the powdered samples. The two-theta starting position was 5 degrees and ended at 80 degrees with a two-theta step of 0.026261 at 30 seconds per step. The Tube current was 40mA and the tension was 45VA. A Programmable Divergent Slit was used with a 5mm Width Mask and the Gonio Scan was used.

The diffracted x-rays intensity was recorded continuously as the sample and detector rotated through their angles respectively. The occurrence of minerals consisting of lattice planes with d-spacings appropriate to the diffracted x-rays at a value of θ results in a peak of intensity. The individual peak has two (2) distinct reflections (Kα1 and Kα2); however, at minor values of 2θ, the peak locations usually overlap with Kα2. This results in a hump-shape on the side of Kα1. Moreover, as the values of θ increase, the separation becomes greater. These combined peaks are usually taken as a single entity. The diffraction peak 2λ position is usually measured as the peak center at 80% peak height.

The results are typically reported as peak positions at 2θ and X-ray counts (intensity) in a tabular format or an x-y plot. Intensity (I) could be reported as the peak's height intensity, (i.e., intensity above background), or as integrated intensity (area beneath the peak). Relative intensity is recorded as the ratio of the peak intensity to that of the most intense peak (relative intensity = I/I1 x 100). The analysis of the samples was conducted at the National Geoscience Research Laboratories, Nigerian Geological Survey Agency, Kaduna South, Kaduna.

Thin section petrography

The thin section was prepared following standard thin section preparation methods including the impregnation of unconsolidated samples using couple of araldites, xylene, molding cup or container. The coupled araldite was mixed in equal proportion with xylene until it formed a semi-solid paste. The inner wall of the molding cup was smeared with Vaseline for easy remover after molding and hardening. The mold was cooled by air drying for a duration of 12 hours to be well solidified before it could be removed from the container. The prepared sample was introduced into a few drops of the prepared cement and stirred uniformly to eliminate air void spaces that formed during the grain packing at the time of formation. The prepared Mold was gently warmed on a hot surface to eliminate bubbles and to hasten hardening. The impregnated sample was smoothened and flattened with coerset carborundum (grinding); firstly, with a fine grit of 600grit carborundum on a glass plate and then followed by 500 grits. The sample was constantly

checked on a microscope to avoid gradual and total scraping of the mineral constituents.

The prepared thin sections were examined under a petrological microscope to identify the mineral assemblages, grain morphology, and other properties while the mineral's optical properties such as cleavage colour, relief, etc. were studied under a Plane polarized Light (PPL) and Cross Polarized light (XPL) of the petrological microscope. The results attained from these analyses were subjected to interpretation to delineate the texture, mineralogical, and modal composition of the rock types being analysed. The slides were studied with the aid of a petrological microscope at the sedimentological laboratory of the Department of Geosciences, University of Lagos.

Result and Discussions

Lithologic sections

The Lokoja sandstone section has a fining upward sequence and consists of a thin layer of conglomerates at the lower section. It reveals lithology of sandstones with different colouration such as cream, white, and purple and the texture of fine, medium, coarse, grain, and matrix-supported conglomerates (Fig. 3). The structures present are trough cross-bedding and lamination. The Patti Formation lithology (Ahoko mine section) includes carbonaceous shales, claystone, and sandstones (Fig. 4). This unit comprises of two (2) distinct members which are the Shale-clay members

(well-bedded shale, claystone, and ironstone) and Sandstone members.

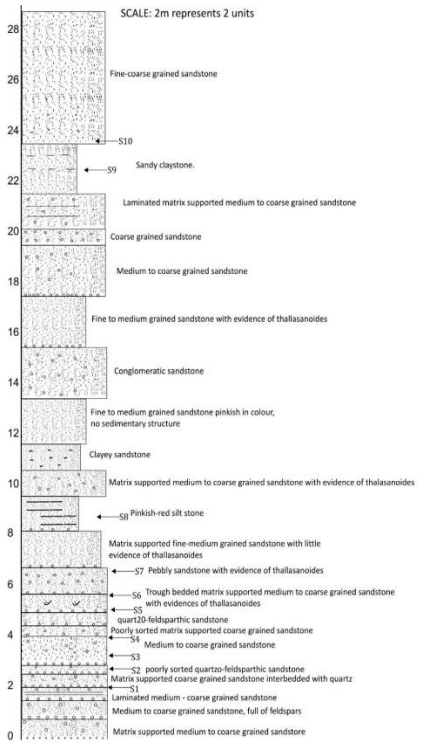

Fig. 3*:* Lithological section of field occurrence of the Lokoja Formation.

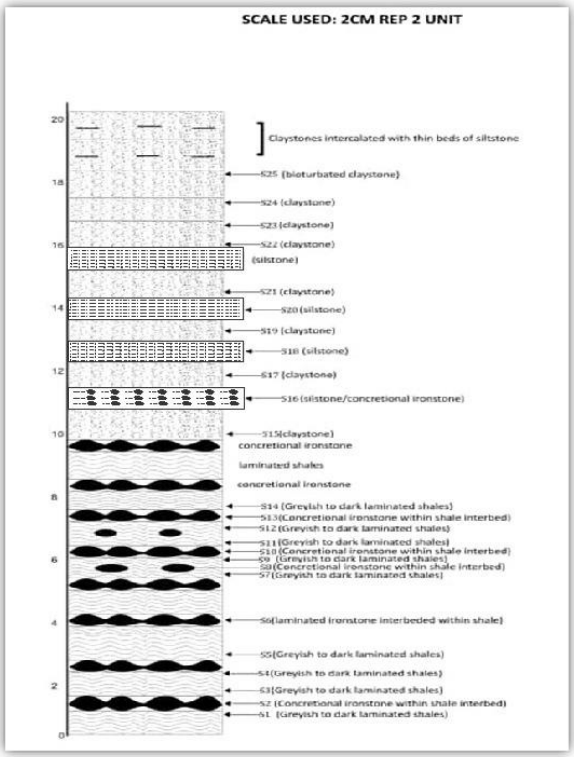

Figure 4: Lithologic Section of the Patti Formation as logged at the Ahoko Mine

Geochemistry

Major Elements Geochemistry

The results of the Major elements are shown in Tables 1-3. The elemental oxides of the Lokoja Sandstone are; 57.34-70.66% SiO_2; 14.11-21.18% Al_2O_3; 1.13-6.17% Fe_2O_3; 0.24-1.36% CaO; 1.92- 3.41% Na_2O; 1.31-3.55% K_2O and 1.91-4.22% MgO. Other oxides such as P_2O_5, TiO_2, and MnO are less than 1% (Table 1). The average composition of the ironstone facies of the Patti in order of abundance are as follows Fe_2O_3 (22.42 – 62.42%), SiO_2 (19.36 – 36.89%), Al_2O_3 (5.39 – 15.35%). Other oxides such as CaO (0.07 – 3.37%), MgO (0.99 – 2.37%) and MnO (1.00 – 2.68%). The shale facie has the abundance of major oxides of SiO_2 > Al_2O_3 > MgO with concentrations 45.80 – 56.82%, 19.46 – 30.50% and 2.14 – 3.84% respectively (Table 3). These oxides accounted for more than seventy percent (70%) of the Shale's elemental oxides. The oxides: P_2O_5 (0.00 – 0.63%), Cl (0.01 – 0.03%), CaO (0.01 – 0.10%w) are relatively low (Table 3)

Table 1: Major Elemental Oxide Composition for the Lokoja Sandstone.

Rock type/ Oxides (wt.%)	FL-S1	FL-S3	OC-S1	OC-S3	OC-S5	0C-S7	OC-S8	OC-S9	OC-S10	OH-S1	OH-S2	OH-S4	OH-S5	Average
SiO_2	58.78	60.41	62.073	67.93	68.09	70.66	58.25	54.59	59.26	57.34	62.81	63.08	61.09	61.87
Al_2O_3	15.45	19.07	17.11	14.29	14.41	14.16	15.11	20.82	19.8	21.18	18.04	14.11	18.14	17.05
Fe_2O_3	4.1	5.92	1.57	1.13	2.54	1.23	6.17	4.33	3.08	1.9	2.27	4.88	3.76	3.30
MgO	1.96	2.75	4.22	2.02	1.91	2.08	3.85	1.83	2.26	2.3	3.11	2.63	2.15	2.54
CaO	0.34	0.28	0.53	0.59	1.16	0.68	1.36	0.29	0.24	0.45	0.97	0.65	0.69	0.63
Na_2O	2.01	3.21	3.02	1.99	1.23	2.45	2.76	3.41	2.84	1.84	2.56	2.32	1.92	2.43
K_2O	1.75	1.32	3.11	3.55	2.59	2.56	1.36	1.32	2.45	1.66	1.31	2.35	1.83	2.09
TiO_2	0.36	0.54	0.16	0.2	0.36	0.25	0.35	0.54	0.26	0.51	0.46	0.43	0.47	0.38
P_2O_5	0.07	0.15	0.11	0.15	0.11	0.13	0.07	0.11	0.12	0.16	0.08	0.11	0.08	0.11
MnO	0.05	0.06	0.04	0.04	0.09	0.04	0.06	0.06	0.05	0.04	0.04	0.05	0.038	0.05
LOI	15.28	6.2	8.47	7.58	7.79	5.5	10.96	12.47	9.59	13.02	8.36	9.88	10.35	9.65
TOTAL	99.81	99.63	99.88	98.88	99.12	99.06	98.94	99.48	99.71	99.95	99.04	99.84	99.83	99.48
SiO_2/Al_2O_3	3.81	3.17	3.63	4.75	4.73	4.99	3.86	2.63	3.00	2.72	3.48	4.47	3.368	3.74
K_2O/Na_2O_3	0.87	0.41	1.03	1.78	2.11	1.05	0.49	0.39	0.86	0.90	0.51	1.01	0.95	0.95
KvO/Al_2O_3	0.11	0.07	0.18	0.25	0.18	0.18	0.09	0.06	0.12	0.08	0.073	0.17	0.10	0.13
Al_2O3/TiO_2	42.92	35.31	106.94	71.45	40.03	56.64	43.17	38.56	76.15	41.53	39.22	32.81	38.60	51.03
$Log(K_2O/Na_2O)$	-0.06	-0.39	0.01	0.25	0.32	0.02	-0.31	-0.41	-0.06	-0.04	-0.29	0.01	-0.02	-0.08
$Log(SiO_2/Al_2O_3)$	0.58	0.50	0.56	0.68	0.67	0.70	0.59	0.42	0.48	0.43	0.54	0.65	0.53	0.57
CIA (%)	79.03	79.86	71.98	69.98	74.32	71.34	73.39	80.57	78.17	84.28	78.85	72.62	80.34	76.52
CIW (%)	86.80	84.53	82.83	84.71	85.77	81.90	78.58	84.91	86.54	90.24	83.63	82.61	87.42	84.65
PIA (%)	86.80	84.53	82.82	84.71	85.77	81.90	78.58	84.91	86.54	90.24	83.64	82.61	87.422	84.78
ICV (%)	29.36	26.07	79.06	47.60	27.44	37.16	45.46	21.82	43.0	17.06	23.30	30.95	23.106	30.36
MIA (%)	58.06	59.72	43.96	39.96	48.63	42.67	46.77	61.15	56.34	68.56	57.69	45.24	60.673	53.03

Table 2: Major Oxides Composition of Ironstone samples

	AH-S2	AH-S6	AH-S8	AH-S10	AH-S13	AH-S16	SUM	MEAN
Fe_2O_3	31.17	37.96	22.42	26.84	28.61	62.42	209.42	34.90
MgO	1.66	1.83	2.37	1.65	1.7	0.99	10.2	1.70
Al_2O_3	6.47	13.72	9.75	7.55	15.35	5.39	58.23	9.71
SiO_2	29.22	19.36	36.89	34.11	28.3	25.46	173.34	28.89
P_2O_5	0.29	0.14	0	0.24	0.27	0.83	1.77	0.30
SO_3	0.63	0.59	1.43	0.22	0.64	0.03	3.54	0.59
Cl	0.04	0.07	0.05	0	0.04	0.03	0.23	0.04
K_2O	0.4	0.46	0	1	0.69	0.22	2.77	0.46
CaO	1.22	3.37	1.39	1.73	1.68	0.07	9.46	1.58
TiO_2	0.95	0.46	0.58	1	1.21	0.45	4.65	0.78
Na_2O	0.01	0	0	0	0.02	0	0.03	0.01
V_2O_5	0.03	0.04	0.02	0.03	0.03	0.04	0.19	0.03
Cr_2O_3	-	0.01	-	-	0	0	0.01	0.00
MnO	2.51	2.2	1.08	1	2.68	1.28	10.75	1.79
SrO	0.73	0.71	0.71	0.71	0.71	0.7	4.27	0.71
ZrO_2	-	-	-	0.03	0.05	-	0.08	0.04
Bi_2O_3	-	-	0.04	-	-	0	0.04	0.02
la_2O_3	0.35	0.76	0.41	-	-	0.71	2.23	0.56
BaO	-	0.08	-	0.05	-	0	0.13	0.04
ZnO	-	0.01	0.01	0.01	-	0.01	0.04	0.01
As_2O_3	-	-	-	0.01	0.002	0	0.012	0.00
L.O.I.	24	20	22	23.8	18	1	108.8	18.13
TOTAL	**99.68**	**101.77**	**99.15**	**99.98**	**99.983**	**99.631**		

Table 3: Major Oxides Composition of Shale Samples (Patti Formation)

	AH-S1	AH-S4	AH-S7	AH-S9	AH-S12	AH-S14	SUM	MEAN
Fe_2O_3	2.04	2.59	4.19	2.04	0.54	2.16	13.56	2.26
MgO	3.75	3.23	3.50	3.75	2.14	3.84	20.21	3.37
Al_2O_3	22.99	30.50	25.06	22.99	19.46	23.43	144.43	24.07
SiO_2	51.04	45.80	47.54	51.04	56.82	50.09	302.33	50.39
P_2O_5	0.25	0.63	0.22	0.25	0.00	0.26	1.61	0.27
SO_3	1.31	0.71	2.27	1.31	0.23	1.35	7.18	1.20
Cl	0.03	0.02	0.03	0.03	0.01	0.01	0.13	0.02
K_2O	1.28	1.07	0.94	1.28	1.00	1.13	6.70	1.12
CaO	0.03	0.10	0.07	0.03	0.01	0.03	0.27	0.05
TiO_2	1.67	1.27	1.61	1.67	1.34	1.95	9.51	1.59
Na_2O	0.03	0.03	0.04	0.03	0.01	0.04	0.18	0.03
V_2O_5	0.03	0.05	0.07	0.03	0.01	0.04	0.23	0.04
Cr_2O_3	0.01	0.02	0.02	0.01	0.05	0.01	0.12	0.02
MnO	0.08	0.12	0.00	0.00	3.00	0.09	3.29	0.55
CeO_2	3.00	0.00	0.00	3.00	0.72	0.00	6.72	2.24
SrO	0.72	0.16	0.73	0.72	0.72	0.73	3.78	0.63
ZrO_2	0.32	0.11	0.00	0.00	0.61	0.45	1.49	0.37
PbO	0.01	0.02	0.00	0.01	0.01	0.01	0.06	0.01
Bi_2O_3	0.04	0.04	0.00	0.00	0.00	0.04	0.12	0.04
Ga_2O_3	0.00	0.01	0.01	0.00	0.00	0.00	0.02	0.01
NiO	0.00	0.01	0.02	0.00	0.00	0.00	0.03	0.02
Ta_2O_5	0.00	0.01	0.02	0.01	0.01	0.01	0.06	0.01
WO_3	0.00	0.01	0.02	0.01	0.01	0.01	0.06	0.01
L.O.I.	12.20	13.00	14.00	12.00	13.80	13.90	78.90	13.15
TOTAL	**100.83**	**99.52**	**100.49**	**100.23**	**100.51**	**99.61**		

The Al_2O_3/Ti_2O ratio of the Lokoja sandstones (32.81 - 106.94) suggests intermediate to felsic source rocks (Hayashi et al., 1997).

The authors suggested that Al_2O_3/ Ti_2O ratio increases from 3 - 8 for mafic igneous rocks, 8 - 21 for intermediate rocks, and 21 - 70 for felsic igneous rocks.

The potassium oxide (K_2O) content – (1.31.-3.55) with an average value of 2.09, which is > unity (1) indicates slightly enriched K-feldspar or illite (Akpokodje *et al.*, 1991; Okunlola and Idowu, 2012).

The recorded low K_2O concentration (0 – 0.69% of the ironstone facies indicates the possibility of a low occurrence of illite or K-feldspar presence as observed in the XRD results while the the low K_2O concentration (0.94 – 1.28%) indicates low concentration of illite or K-feldspar present and absence of expendable clays like smectite or montmorillonite.

Cross plots of % SiO_2 versus $\%Fe_2O_3$ (Fig.5a); $\%SiO_2$ versus $\%Al_2O_3$ (Fig. b) and $\%SiO_2$ versus %LOI (Fig. 5c) all indicate a negative correlation. These demonstrate the influence of weathering processes through the enrichment of silica and depletion of Fe and Mg as well as the decrease in LOI with increasing weathering and maturity of the sediments. The negative correlation between SiO_2 and Al_2O_3 is also an indication of the fact that most of the silica is present as quartz grains (Tijani et al., 2010).

However, the positive correlation between Fe_2O_3 and Al_2O_3 (Fig. 5d) is an indication of a common source.

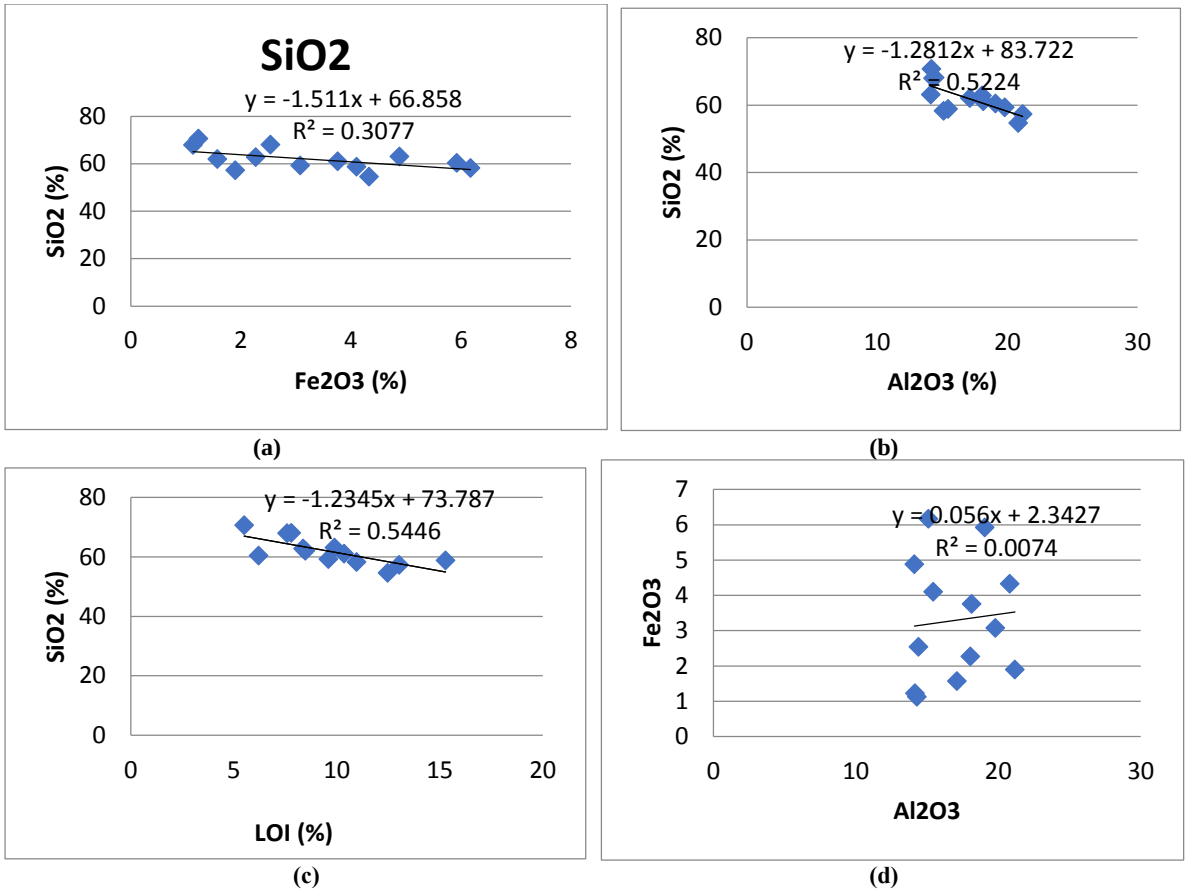

Fig. 5: Cross Plots of Major Oxides: (a) SiO_2 against Fe_2O_3, (b) SiO_2 against $A1_2O_3$, (c) SiO_2 against LOI, (d) Fe_2O_3 against $A1_2O_3$

Mineralogy of Ironstone and Shales

The ironstone facies samples of the Patti Formation indicate the occurrence of Siderite (Fe_2CO_3), Kaolinite (Al_2O_3 $2SiO_2{\cdot}2H_2O$), Quartz (SiO_2), and Hematite (Al_2O_3) as shown in table 4 and figures 6 to 7. The results revealed that Siderite, kaolinite, and quartz formed the bulk composition (about 75.2%) of the sample. Siderite had the largest concentration across the samples ranging from 40 – 61% with an average of 43%. Kaolinite had the second largest proportion ranging from 26% - 36% while averaging 26%. Quartz had a concentration ranging from 6% - 28% with an average of 18%.

The results revealed that kaolinite and quartz formed the bulk composition (about 90%) of the shale sample. Kaolinite had the largest concentration ranging from 25 – 81% with an average of 54%. Generally, Kaolinite is a by-product of chemical weathering (feldspar hydrolysis) in the tropics. Therefore, its abundance suggests a high degree of weathering at the source area. Quartz had the second-highest concentration ranging from 19% - 75% with an average of 44%. However, Hematite and Sylvite had the lowest contributions with an average of 1%.

Table 4: Mineral Constituents of the Ironstone Samples

Mineral	AH-S2	AH-S6	AH-S8	AH-S10	AH-S13	AH-S16	Ave.
Siderite (Fe_2CO_3)	51%	61%	52%	55.60%	40%	-	43
Kaolinite (Al_2O_3 $2SiO_2{\cdot}2H_2O$)	30%	33%	29%	26.30%	36%	-	26
Quartz (SiO_2)	19%	6%	11%	18.20%	24%	28%	18
Hematite (Al_2O_3)	-	-	8%	-	-	72%	13
TOTAL	**100%**	**100%**	**100%**	**100%**	**100%**	**100%**	

Table 5: Mineral Constituents of the Shale Samples

Mineral	AH-S1	AH-S4	AH-S7	AH-S9	AH-S12	AH-S14	Ave.
Kaolinite (Al_2O_3 $2SiO_2 \cdot 2H_2O$)	81%	61%	68%	44%	45%	25%	54%
Quartz (SiO_2)	19%	39%	23%	53%	55%	75%	44%
Hematite (Al_2O_3)	0	0	7%	0%	0	0	1%
Sylvite (KCl)	0	0	2%	3%	0	0	1%
TOTAL	**100%**	**100%**	**100%**	**100%**	**100%**	**100%**	

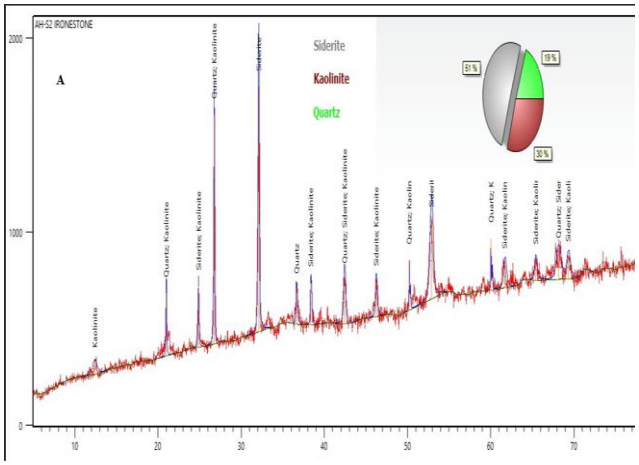

Fig.6a: XRD diffractogram of Ironstone sample AH-S2 showing peaks for Siderite, Kaolinite, and Quartz

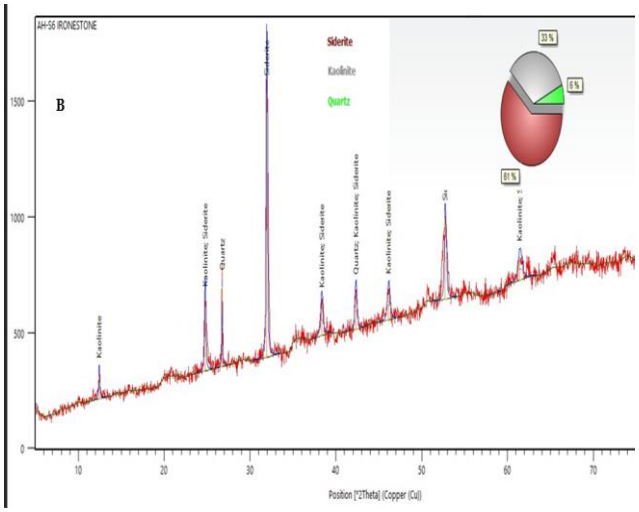

Fig. 6b. XRD diffractogram of Ironstone sample AH-S6 showing peaks for siderite, kaolinite

and quartz

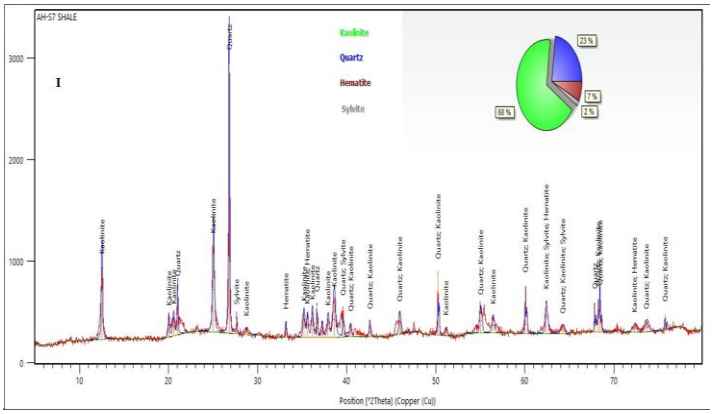

Fig. 7a: XRD diffractogram of Shale sample AH-S7 showing peaks for Kaolinite, Quartz, Hematite, and Sylvite

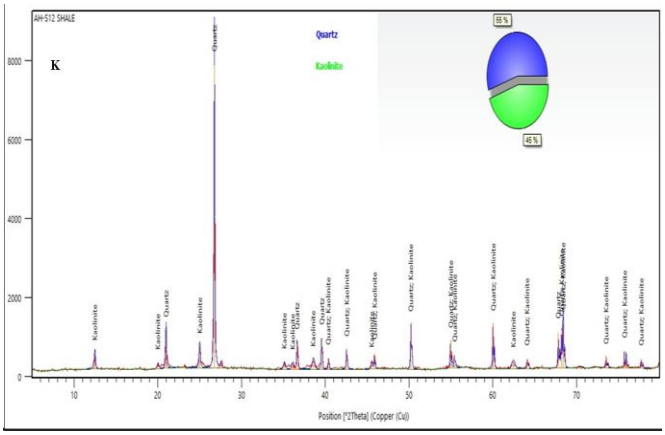

Fig. 7b: XRD diffractogram of Shale sample AH-S12 shows peaks for Quartz and Kaolinite.

Petrography of the Lokoja Sandstone

The result of the sandstone petrography is shown in Table 6 and figure 8. The framework grains of the sandstone is dominantly composed of sub-angular to sub-rounded monocrystalline quartz. There are also substantial amounts of feldspars and lithic fragments. The feldspars are mainly microcline with minor plagioclase.

The substantial quantity of feldspar and the low abundance of rock fragments in the studied samples indicate that the sandstone under investigation is mineralogically immature.

Table 6: Petrographic Analysis Data Showing Total and Framework Composition of Sandstone in the Study Area.

Sample No.	Quartz	Feldspar	Rock Fragment	Mica	Matrix/Cement	Framework Composition (%)			
						Q	F	RF	MMI
FL-S1	68	10	5	2	15	81.93	12.05	6.02	4.53
FL-S3	57	12	10	3	18	72.15	15.19	12.66	2.59
FL-S5	64	5	9	5	17	82.05	6.41	11.54	4.57
OC-S1	54	20	8	3	15	65.85	24.39	9.76	1.92
OC-S2	63	15	5	2	15	75.90	18.07	6.03	3.15
OC-S3	63	15	5	2	15	75.90	18.08	6.02	3.15
OC-S4	45	30	7	3	15	54.88	36.58	8.54	1.22
OC-S5	57	25	5	1	12	65.53	28.74	5.73	1.90
OC-S6	53	23	4	5	15	66.25	28.75	5.00	1.96
0C-S7	61	15	11	3	10	70.12	17.24	12.64	2.35
OC-S8	53	25	5	2	15	63.86	30.12	6.02	1.77
OC-S9	52	20	9	1	18	64.20	24.69	11.11	1.79
OC-S10	45	20	15	5	15	56.25	25.00	18.75	1.29
OH-S1	46	25	10	4	15	56.79	30.86	12.35	1.31
OH-S2	56	15	8	3	18	70.88	18.99	10.13	2.43
OH-S3	58	15	5	2	20	74.36	19.23	6.41	2.90
OH-S4	58	18	8	1	15	69.05	21.43	9.52	2.23
OH-S5	60	15	10	3	12	70.59	17.65	11.76	2.40
OH-S6	56	10	10	4	20	73.68	13.16	13.16	2.80
OH-S7	56	10	13	3	18	70.89	12.65	16.46	2.44
Average	56.25	17.15	8.1	2.85	15.65	69.02	21.04	9.94	2.23

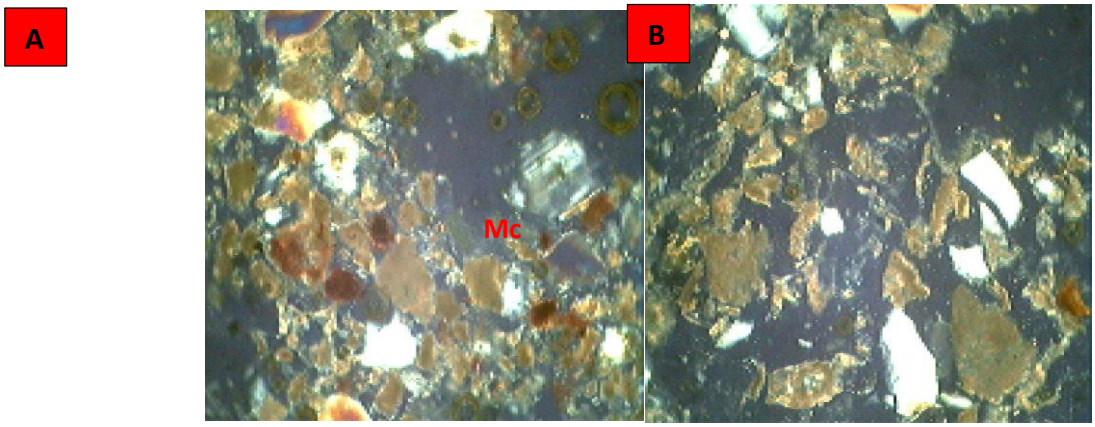

Fig.8: Photomicrograph of Sandstone of Lokoja Formation (A and B; cross nicol, mag = 40x) characterized by Angular grains of Quartz and Feldspar

Based on Folk's (1974) classification scheme, which completely discards matrix as an important element in sandstone classification, the Lokoja Sandstone is classified as an arkosic or feldsparthic arenite (Fig. 9).

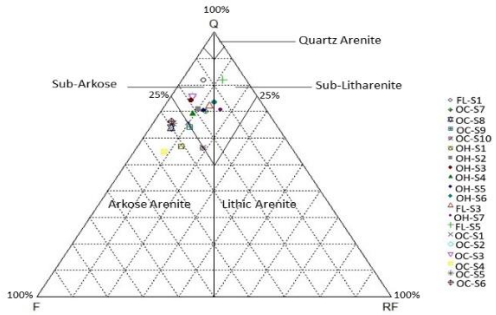

Fig. 9: QFRF Ternary Diagram for Sandstone-Mineral Base Classification for Study Area, (After Folk, 1974). Note Q = Total Quartz, F = Feldspar and RF = Rock Fragments

Provenance

According to Taylor and Mclennan, (1985); Condie et al, (1992); and Madhavaraju et al. (2016), clastic sediments geochemical signatures can be used to determine their provenance characteristics. The Al_2O_3/TiO_2 ratio could be used to infer the source rock composition in several clastic sediments. According to Hayashi et al. (1997), when the Al_2O_3/TiO_2 ratios range from 3 – 8, it suggests mafic igneous rocks, 8 - 21 suggests intermediate rocks while a range of 21 - 70 represents felsic igneous rocks. The results of the studied shale samples Al_2O_3/TiO_2 ratios range from 12.02 – 24.02 (Average; 15.61). This suggests a mixture of felsic igneous and an intermediate igneous rock as the source rock for the shale samples. Furthermore, the bivariate plot of Al_2O_3/TiO_2 vs. SiO_2 by Le Bas et al. (1986) can also be used to discriminate source rock's provenance as felsic, intermediate, and mafic provenance. Here, the investigated shale sediments are plotted within the mafic and intermediate fields (Fig.10). This suggests that the contributions were from both sources.

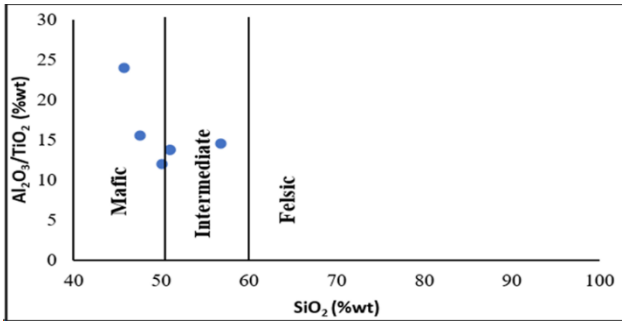

Fig.10: Shale samples bivariate Plot for Al2O3/TiO2 vs. SiO2 by Le Bas et al. (1986)

Also, the Al_2O_3/TiO_2 ratio was used to infer the ironstone source rock composition. The ratio ranged from 6.81 – 29.83 with an average of 14.28. This suggests a mix of mafic and intermediate provenance for the ironstone samples. However, the bivariate plot of Al_2O_3/TiO_2 vs. SiO_2 revealed a purely mafic source provenance (Fig.11) for the studied ironstones. The Roser and Korsch (1988) discriminant function plot was used to infer the provenance of the shale samples using their major elemental oxides composition. The ironstone samples plotted within the Mafic igneous provenance i.e. first-cycle basaltic and lesser andesitic detritus (Fig.12) while the plotted Lokoja sandstone were deposited in the oceanic island arc provenance field while in the discrimination diagram; it plotted the sandstones in the Quartzose sedimentary provenance (Fig.13)

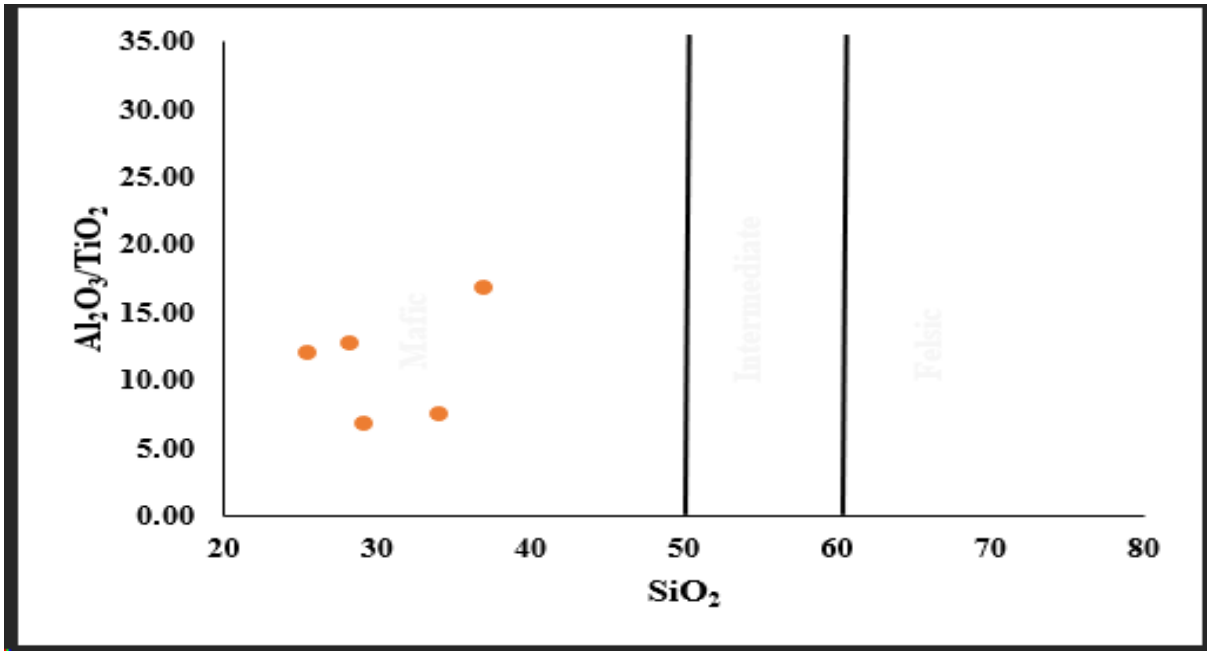

Fig. 11: Bivariate Plot for Al2O3/TiO2 vs. SiO2 by Le Bas et al., (1986) of the Ironstone samples

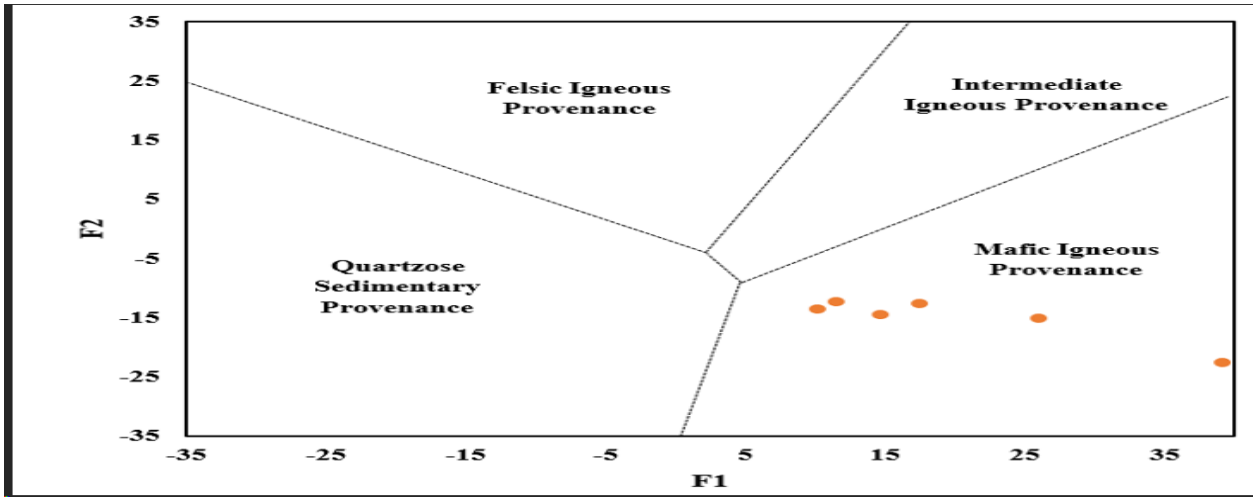

Fig. 12: Provenance of Ironstone samples using Discriminant Function diagram of Roser and Korsch (1988

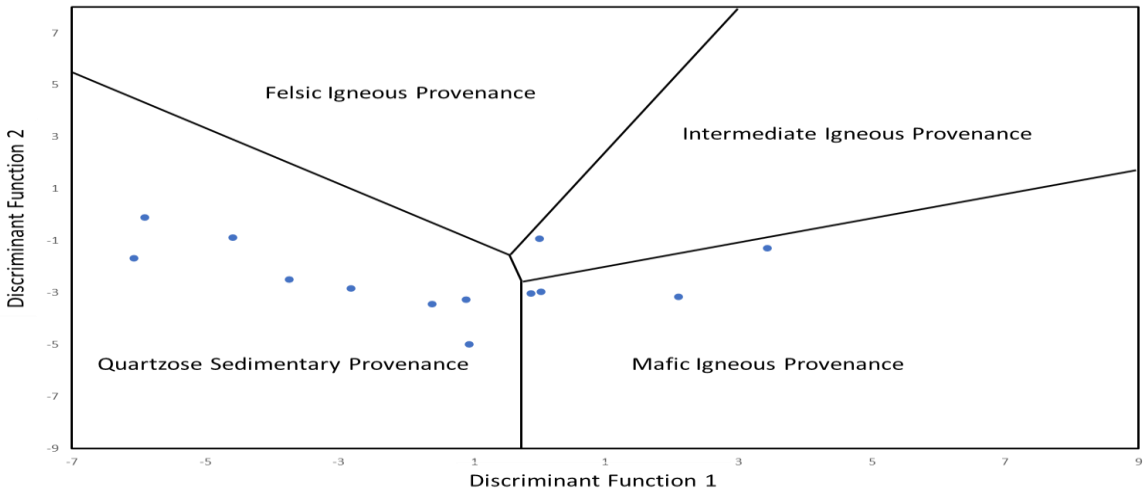

Fig. 13: Tectonic Discrimination Plot for the Lokoja Sandstone (After Roser and Korsch, 1986).

Tectonic Settings

The tectonic setting of the ironstone samples was determined with the use of the Tectonic Discriminant Diagram for sediments (After Roser and Korsch, 1986). It involved the bivariate plot of log K_2O/Na_2O against SiO_2 (Fig.14). The result revealed that the ironstone samples plotted within the Active Continental Margin (ACM).

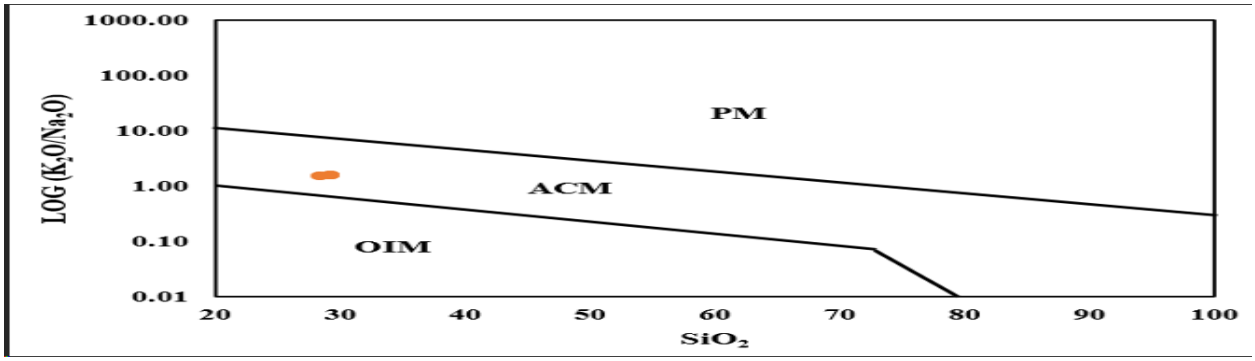

Fig.14: Tectonic Discriminant Diagram for Ironstone samples (After Roser and Korsch, 1986); ACM: Active Continental Margin; PM: Passive Margin; CIA: Continental Island Arc; OIA: Oceanic Island Arc

The plot (K_2O/Na_2O) vs SiO_2 for the shale is depicted in figure 15. The plot reveals that the shale sediments plot entirely in the Active Continental Margin. Similar plot of (K_2O/Na_2O) vs SiO_2 for the Lokoja Sandstone (Fig. 16) shows Active Continental Margin (ACM) and Continental Island Arc (CIA), although, majority plotted into the oceanic island arc classification.

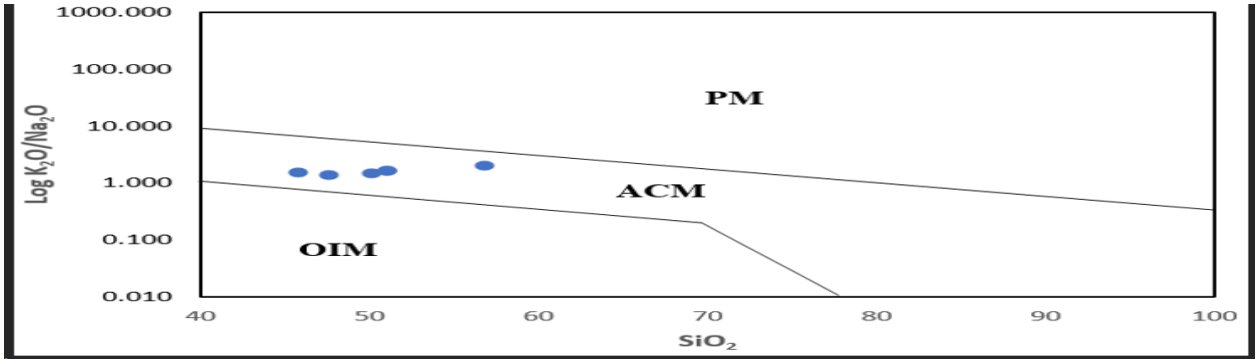

Fig.15: Tectonic Discriminant Diagram for Shale sediments (After Roser and Korsch, 1986)

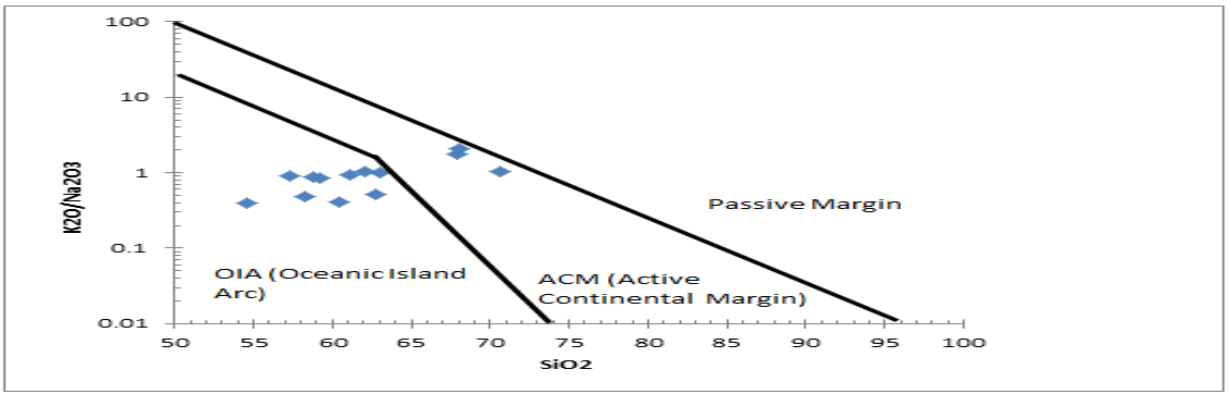

Fig.16: Tectonic Discrimination Plot for the Lokoja Sandstone (After Roser and Korsch, 1986).

Conclusion

The composition, provenance and tectonic setting of the Lokoja (Sandstone) and Patti Formations (Ironstone and Shale) has been assessed using geochemical and petrographic approaches. The Al_2O_3/Ti_2O ratio range for the sandstones (32.81 - 106.94) suggests intermediate to felsic source rocks and the sandstone was classified as greywacke. The low K_2O concentration of the ironstone and shale facies indicates the possibility of a low occurrence of illite or K-feldspar presence as observed in the XRD results. The Al_2O_3 /TiO_2 ratio suggests a mix of mafic and intermediate provenance for the ironstone samples, it suggest the shale provenance to be a mixture of felsic igneous and an intermediate igneous rock, while it suggest the Lokoja sandstone to be of a Quartzose sedimentary provenance.

The tectonic setting was determined with the use of the Tectonic Discriminant Diagram. It revealed the ironstone and shale facies of the Patti Formation plotted within the Active Continental Margin (ACM), whereas, the Lokoja sandstone samples majorly plotted within the Oceanic Island Arc (OIA) with few on them within the Active Continental Margin (ACM). Chemical Index of Alteration (CIA) revealed that the Ironstone and Shale facies of the Patti Formation have undergone extreme weathering in the source area under semi-humid to semi-arid conditions and the samples are chemically immature.

Acknowledgements

The authors are grateful to Mr. Nura Adamu Mohammed of the Research Laboratories, Nigerian Geological Survey Agency, Kaduna South for the XRF & XRD analysis. Mr. Olagbaju of the geological Laboratory, University of Lagos, Nigeria for his support during the thin sectioning analysis.

References

Abimbola, A.F. 1997. Petrographic and paragenetic studies of the Agbaja Ironstone Formation, Nupe Basin, Nigeria. Journal of African Earth Sciences, 25, 169-181.

Adeleye, D. R. (1973). Origin of ironstones, an example from the Middle Niger Vallley, Nigeria. Journal Sedimentary Petrology, 43, 709-727.

Agunleti Y. S. and Salau S. L. (2015). Geochemical Studies and Exploration Potential of The Oolitic-Pisolitic Ironstone Deposits Of Agbaja Formation Southern Bida Basin North-Central Nigeria International Journal of Innovative Science, Engineering & Technology, 2(5), 527 – 533.

Agyingi, C.M., 1991: Geology of Upper Cretaceous rocks in

the eastern Bida, Nigeria. Unpublished Ph.D. Thesis, department of Geology, University of Ibadan, 501pp.

Akande, S. O., Ojo, O. J., Erdtmann B.D. and Hetenyi, M. A. (2005). Paleoenvironments, organic petrology and Rock-Eval studies on source rock facies of the Lower Maastrichtian Patti Formation, southern Bida Basin, Nigeria. Journal of African Earth Sciences, 41(5), 294-406.

Akpokodje, E. G., Etu-Efeotor, J. O. and Olorunfemi, B.N. (1991). The composition and Physical Properties of some Ceramic and Pottery Clays of South Eastern Nigeria. Journal of Mining and Geology, 27, 9 – 15.

Bankole, S. I. Akinmosin, A., Omeru, T. and Ibrahim, H. E. (2019). Heavy mineral distribution in the Lokoja and Patti Formations, Southern Bida Basin, Nigeria: Implications for provenance, maturity and transport history. RMZ, DOI: 10.2478/rmzmag-2019-0011

Braide, S. P. (1992). Geologic development, origin and energy mineral resources potential of the Lokoja Formation in the sourthern Bida Basin. Journal of Mining Geology, 28, 33–44.

Condie, K. C., Boryta, M. D., Liu, J. and Quian, X. (1992). The origin of khondalites: geochemical evidence from the Archean to Early Proterozoic granulitic belt in theNorth China Craton: Precambrian Research, 59(3-4), 207 – 223

Folk, R. L. 1974.Petrology of sedimentary rocks. Hemphil, Austin, Texas, 182pp

Hayashi, K., Fujisawa, H., Holland, H., Ohmoto, H. (1997). Geochemistry of 1.9 Ga sedimentary rocks from northeastern Labrador, Canada: Geochimicaet Cosmochimica Acta, 61(19), 4115-4137.

Jones H. A. (1958). The Oolitic Ironstones of Agbaja Plateau, Kabba Province. Record of the Geological Survey of Nigeria, 20–43

Ladipo K. O., Akande S. O., A. Mücke (1994). Genesis of ironstones from the Middle Niger sedimentary basin, evidence from ore microscopic and geochemical studies. J. Min. Geol., 30, 161-168

Le Bas M. J., Le Maitre R. W., Streckeisen, A. and Zanettin, B. (1986). A chemical classification of volcanic rocks based on the total alkali-silica diagram. Journal of Petrology, 27, 745–750.

Madhavaraju, J., Ramirez-Montoya, E., Monreal, R., Gonzalez–Leon, C. M., Pi-Puig, T., Espinoza-Maldonado, I. G. and Grijalva–Noriega, F. J. (2016). Paleoclimate, paleo weathering and paleo-redox conditions of Lower Cretaceous shales from the Mural Limestone, Tuape section, northern Sonora, Mexico: Constraints from clay mineralogy and geochemistry. Revista Mexicana de Ciencias Geologicas, 33(1), 34- 691.

Nton M. E. and Adamolekun O. J. (2016). Sedimentological and Geochemical characteristics of outcrop sediments of Southern Bida Basin, Central Nigeria: Implications for provenance, paleoenvironment and tectonic history. Ife Journal of Science, 18(2), 345 – 369

Obaje, N. G., Wehner, H. and Scheeder, G. (2004). Hydrocarbon prospectivity of Nigeria's inland basins from the viewpoint of organic geochemistry and organic petrology. American Association of Petroleum Geologists Bulletin, 88, 325 – 353.

Obaje N.G., Musa, M. K., Odoma A.N., and H. Hamza H. (2011) "The Bida Basin in North-Central Nigeria: sedimentology and petroleum geology" Journal of Petroleum and Gas Exploration Research,1(1), 001-013.

Ojo, O. J. and Akande, S.O., (2008). Microfloral assemblage, age and paleoenvironment of the Upper Cretaceous Patti Formation, southeastern Bida Basin, Nigeria: Journal of.Mining and Geology, 44, 71- 78.

Okunlola, O.A. and Idowu, O. (2012). The geochemistry of claystone-shale deposits from the Maastritchian Patti Formation, Southern Bida Basin, Nigeria. Earth Sci. Res. SJ, 16 (2): 57 – 67

Roser, B.P. and Korsch, R.J. (1986). Determination of tectonic setting of sandstone mudstone suites using SiO content and 2 KO/NaO ratio. Jour. Geol. 94, 635–650

Roser, B.P., and Korsch, R.J. (1988). Provenance signatures of sandstone–mudstone suites determined using discriminant function analysis of major-element data: Chemical Geology, 67, 119-139.

Taylor, S. R., and McLennan, S. M. (1985). The Continental Crust: its composition and evolution: An examination of the geological record preserved in sedimentary rocks: Oxford, U.K., Blackwell, 328 pp.

Tijani, M. N., Nton, M. E., Kitagawa, R. (2010). Textural and geochemical characteristics of the Ajali Sandstone, Anambra Basin, SE Nigeria: Implication for its provenance. Comptes Rendus Geoscience, 342, 136–150.